Contents lists available at ScienceDirect

Toxicology Reports

Pharmacokinetic analysis of acute and dietary exposure to piperonyl butoxide in the mouse

Alyssa E. Jenkins [a], Cameron O. Scarlett [b], Tyler G. Beames [a], Kenneth S. Rivera-González [a], Alexander A. Martin [a], Miranda R. Sun [a], Paul R. Hutson [b,*], Robert J. Lipinski [a,**]

[a] *Department of Comparative Biosciences, School of Veterinary Medicine, University of Wisconsin-Madison, Madison, WI 53706, USA*
[b] *School of Pharmacy, University of Wisconsin-Madison, Madison, WI 53705, USA*

ARTICLE INFO

ABSTRACT

Piperonyl butoxide (PBO) is a popular insecticide synergist present in thousands of commercial, agricultural, and household products. PBO inhibits cytochrome P450 activity, impairing the ability of insects to detoxify insecticides. PBO was recently discovered to also inhibit Sonic hedgehog signaling, a pathway required for embryonic development, and rodent studies have demonstrated the potential for *in utero* PBO exposure to cause structural malformations of the brain, face, and limbs, or more subtle neurodevelopmental abnormalities. The current understanding of the pharmacokinetics of PBO in mice is limited, particularly with respect to dosing paradigms associated with developmental toxicity. To establish a pharmacokinetic (PK) model for oral exposure, PBO was administered to female C57BL/6J mice acutely by oral gavage (22–1800 mg/kg) or via diet (0.09 % PBO in chow). Serum and adipose samples were collected, and PBO concentrations were determined by HPLC-MS/MS. The serum concentrations of PBO were best fit by a linear one-compartment model. PBO concentrations in visceral adipose tissue greatly exceeded those in serum. PBO concentrations in both serum and adipose tissue decreased quickly after cessation of dietary exposure. The elimination half-life of PBO in the mouse after gavage dosing was 6.5 h (90 % CI 4.7–9.5 h), and systemic oral clearance was 83.3 ± 20.5 mL/h. The bioavailability of PBO in chow was 41 % that of PBO delivered in olive oil by gavage. Establishment of this PK model provides a foundation for relating PBO concentrations that cause developmental toxicity in the rodent models to Sonic hedgehog signaling pathway inhibition.

1. Introduction

Piperonyl butoxide (PBO) is a pesticide synergist that acts by inhibiting cytochrome P450 (CYP) enzymes, resulting in delayed breakdown of pyrethrum and synthetic pyrethrin insecticides in the target organism [1]. Developed in the 1940s, PBO is now a popular pesticide synergist present in over 2500 commercial, agricultural, and home-use products [2,3]. Reproductive and developmental toxicity assessments have yielded mixed results, with studies in multiple species finding limited or no evidence for PBO teratogenicity [1,4–7]. However, several rodent studies have linked prenatal PBO exposure to overt malformations of the brain, face, and limbs, or more subtle postnatal behavioral alterations [8–12].

PBO was recently discovered to inhibit the Sonic hedgehog (Shh) signaling pathway through a mechanism distinct from CYP modulation [13]. The Shh signaling pathway plays critical roles in embryogenesis, including development of the brain, face, and limbs [14]. Studies in mice and rats have demonstrated a potential for acute administration of PBO by oral gavage to cause limb malformations [9,11]. In a separate mouse study, oral gavage administration of PBO targeted to an earlier critical period of development was found to result in abnormal development of the brain and face, with the outcomes ranging from subtle dysmorphology to overt malformations with increasing dose [8]. The malformations of the brain, face, and limbs found to result from *in utero* PBO exposure are consistent with Shh pathway disruption and closely approximate those reported to result from exposure to a highly potent and specific Shh pathway inhibitor at parallel developmental stages in mice [15]. Additional studies have also linked PBO exposure to more subtle adverse neurodevelopmental impacts. In two mouse-based studies, dietary PBO exposure targeting gestation and lactation

---

resulted in behavioral differences in PBO-exposed versus control offspring [10,12]. Collectively, these studies established the potential for oral PBO exposure to cause adverse developmental outcomes in rodents, with the specific outcome appearing to be dependent upon dose, route, and timing of exposure.

Human exposure to PBO is widespread and occurs through multiple sources. PBO is detected in produce, livestock, surface water, and household dust [16–18], suggesting that oral exposure may be a significant exposure route. Our understanding of PBO pharmacokinetics (PK) is limited, and apart from being detected in human umbilical cord fluid [19], to our knowledge PBO serum concentrations in humans have not been reported. Results from a study of four male volunteers suggest that dermal absorption is minimal over an eight-hour period [20]. Early rodent studies suggested that PBO is readily absorbed when administered orally [21,22]. A PK study of oral PBO exposure in male rats found that PBO concentrations in brain, testis, liver, and adipose exceeded those detected in plasma [23]. However, this study in rats was limited to examination of a single route of administration and single dose of PBO, while most studies demonstrating developmental toxicity of PBO were conducted in the mouse, for which little PK data are available.

The aim of the study described herein was to establish a PK model of PBO exposure in the mouse. PBO was administered to wildtype female C57BL/6J mice by oral gavage or through diet to reflect exposure paradigms found to cause developmental abnormalities in previous murine studies. PBO concentrations in serum and adipose tissue were determined by HPLC-MS/MS and used to generate a PK model incorporating mixed-effects methods. By establishing PK profiles for PBO doses associated with adverse developmental outcomes in the mouse, these findings provide a foundation for better understanding human PBO exposure and its potential contribution to adverse developmental outcomes.

2. Materials and methods

2.1. Chemicals

Piperonyl butoxide (PBO) was purchased from Toronto Research Chemicals (North York, Ontario). Purity of > 96 % was verified by HPLC-MS/MS as previously described [8]. PBO was suspended in olive oil (Spectrum Chemical Mfg. Corp., New Brunswick, NJ) prior to delivery by oral gavage. PBO used in diet formulation was suspended in soybean oil (Spectrum Chemical Mfg. Corp., New Brunswick, NJ) prior to inclusion.

2.2. Animals

This study was conducted in compliance with ARRIVE guidelines and in accordance with the recommendations set forth in the *Guide for the Care and Use of Laboratory Animals* of the National Institutes of Health. The experimental protocol was approved by the University of Wisconsin-Madison School of Veterinary Medicine Institutional Animal Care and Use Committee (Protocol No. V005396, approved October 12th, 2022). Non-pregnant female C57BL/6J mice between 8 and 14 weeks of age were sourced from the Jackson Laboratory (Strain No. 000664; Bar Harbor, ME). Animal rooms were maintained at 23 ± 3 °C and 50 ± 20 % humidity with a 12-hour light, 12-hour dark cycle. Animals were group-housed in specific-pathogen-free conditions in disposable, ventilated cages (Innovive, San Diego, CA) and were fed irradiated soy protein-free extruded rodent diet (Catalog No. 2920x; Envigo Teklad, Madison, WI) unless provided PBO-containing chow as described below. Food and water were provided ad libitum. Mice were euthanized by carbon dioxide asphyxiation followed by cervical dislocation.

2.3. Study design

2.3.1. Acute exposure model

Nulliparous non-pregnant female C57BL/6J mice were administered a single dose of 22.22 mg/kg (n = 8), 66.67 mg/kg (n = 8), 200 mg/kg (n = 8), 600 mg/kg (n = 5), or 1800 mg/kg (n = 5) PBO suspended in olive oil via oral gavage. All gavage doses were administered between 8:30 am and 10:30 am. One mouse was dosed by gavage with 22.22 mg/kg daily for 7 days, with blood samples drawn 1, 24, and 48 h after the last dose of PBO. Mice were visually inspected for signs of overt toxicity immediately following dose administration, and again prior to each sample collection. Whole blood was collected via maxillary (antemortem) or cardiac (postmortem) bleed at multiple time points between 0.5 h (30 min) and 192 h following PBO administration.

2.3.2. Dietary exposure model

Mice were singly housed and acclimated for a minimum of 24 h prior to the start of the study period. PBO suspended in soybean oil was used to generate PBO-containing diets prepared by Envigo (Madison, WI) from base diet (Catalog No. 2919; Envigo Teklad). Control chow diet was prepared with soybean oil alone. One hour prior to the onset of the dark cycle, a 0.09 % PBO diet was introduced to non-pregnant female C57BL/6J mice (n = 48). Daily chow consumption was measured by weighing pellets to allow calculation of PBO ingestion. Whole blood was collected via maxillary (antemortem) or cardiac (postmortem) bleed at various time points between 5 and 192 h following the introduction of the diet. PBO-containing diet was removed at the 192-hour (8-day) time point, and a full cage change was performed to remove any remnants of the PBO-treated diet. PBO-containing diet was replaced with standard chow (Catalog No. 2920x; Envigo Teklad) for the remainder of the study period. Whole blood was collected from remaining animals via maxillary (antemortem) or cardiac (postmortem) bleed after the return to untreated diet.

2.4. Sample processing and quantitation

Three sample types were analyzed for PBO concentration: adulterated mouse chow (for PBO content validation), serum from animals treated with PBO, and adipose tissue from animals treated with PBO. To assay PBO concentration in chow, pellets were ground to a fine powder with a clean mortar and pestle. A 0.20 ± 0.01 g sample was weighed on an analytical balance and transferred to a glass vial containing 2 mL 100 % methanol. The mixture was then vortexed for a minimum of 25 min at high speed. Chow extracts were also prepared from unadulterated pellets for calibrators and quality control samples used in quantitative analysis. All chow extracts were stored at − 80 °C until analysis. Immediately before analysis, chow extracts were further diluted with methanol between 1:50 and 1:300 to avoid detector saturation on the mass spectrometer.

Whole blood collected via maxillary (antemortem) or cardiac (postmortem) bleed was allowed to clot at room temperature for 30 ± 10 min before being centrifuged at 4 °C for 20 min at 2000 g. The serum fraction was removed and centrifuged for an additional 2 min at 4 °C and 2000 g. If below a volume of 40 μL, sample serum was brought to volume with untreated CD1 mouse serum (Innovative Research, Novi, MI). Samples were stored in low-retention microfuge tubes at − 80 °C until quantitation.

Visceral adipose was harvested from the gonadal depot immediately following euthanasia and was stored at − 80 °C in three volumes of phosphate-buffered saline. Visceral adipose tissue samples also required processing before quantitative analysis. These samples were thawed on ice and brought up to between three and seven volumes per gram of tissue with phosphate-buffered saline. Samples were then individually extracted using a Fisherbrand 150 homogenizer. Each chilled sample was homogenized at moderate to high speed for ten seconds, returned to ice for ten seconds, then homogenized for an additional ten seconds at the same speed. The tip of the homogenizer was rinsed once with 70 % ethanol, twice with phosphate-buffered saline, and blotted dry between each sample. Extracts were stored on ice until quantitative analysis.

Adipose extracts, chow extracts, and mouse serum were all processed

for protein precipitation and filtration to remove insoluble materials immediately before quantitative analysis. Briefly, 25 μL of sample were added to 100 μL of acidic acetonitrile containing $^2H_9$-piperonyl butoxide (Toronto Research Chemicals, North York, Ontario) internal standard (ITSD) in a Sirocco filtration plate (Waters Corp., Milford MA). Calibrators were prepared in blank matrix at concentrations between 0.3 ng/mL and 1000 ng/mL and processed alongside experimental samples. Quality control samples (QCs) at low, medium, and high concentrations were also prepared in blank matrix and analyzed to ensure assay performance. Samples were mixed and analyzed by HPLC-MS/MS. Samples were injected in triplicate (2 μL per run) on a 2.1 × 100 mm Waters BEH C18 ultra performance liquid chromatography column (UPLC) and separated by a binary gradient generated using a Waters I-Class Acquity UPLC. UPLC conditions and the solvent gradient are summarized in Table 1. Retention time for PBO and the ISTD was ~1.8 min with a clear distinction between the compounds due to the isotope effect. The ammoniated PBO parent ion (356.1 m/z) transitions to product ions 177, 119, and 91 and these were monitored in positive ion mode. The same product ions for the d9-ISTD were monitored. Ions were analyzed in ESI$^+$ mode on a Sciex QTrap 5500. Instrument conditions for analysis were DP 70, ISV 1800, CurG 30, CollG Med, Temp 375, ISG1 22, ISG2 35. For quantitative analysis, the ratio of the unlabeled PBO area under the curve (AUC) to the deuterated internal standard AUC was modeled with a quadratic curve using $1/x^2$ weighting. Calibrators with calculated concentrations outside $\pm$ 15 % of the actual concentration were excluded from the model. For each assay reported, at least three of four QCs at each level were within $\pm$ 15 % of actual concentrations. In these assays no samples with %RSD > 15 % were observed.

2.5. Pharmacokinetics of acute and dietary oral doses of PBO in mice

The final dataset contained 168 evaluable, measurable serum PBO concentrations from 63 mice: postmortem tissue concentrations were collected from 42 animals.

2.5.1. Population pharmacokinetic modeling

Model building and evaluation was conducted using NONMEM Version 7.5 (NONMEM, ICON Development Solutions, Ellicott City, MD), and followed standard model building approaches to define the structure, intersubject variability, and covariate dependence of the model [24,25]. Modeling was performed on a Dell Inspiron 7410 i7 laptop running the current gfortran compiler. R, version 3.2.3 or higher, was used for statistical modeling and creating graphics in combination with XPOSE4 [26]. Wings for NONMEM was used as an interface for the model fitting and bootstrap simulations.

2.5.2. Base model development

The subroutines ADVAN1, ADVAN2, ADVAN3, ADVAN4, and ADVAN6 were used to model 1-, 2-, and 3-compartment models. The first-order conditional estimation (FOCE) with interaction was used. The

Table 1
UPLC-MS/MS column and binary solvent gradient conditions.

Column	Waters UPLC Acquity BEH C18 Column (1.7 μm, 2.1 ×100 mm)				
Column temp. (°C)	28				
Sample temp. (°C)	10				
Solvent A	1 mM ammonium formate and 0.1 % formic acid in 95 % water/5 % acetonitrile				
Solvent B	1 mM ammonium formate and 0.1 % formic acid in 5 % water/95 % acetonitrile				
Time (min)	0	1	2	2.15	2.5
Solvent B (%)	75	98	98	75	75
Total run time (min)	2.5				
Injection volume (μL)	2				
Flow rate	0.35 mL/min				
PBO Retention Time	1.8 min				

samples were separated into two groups. The animals who received the PBO at a known time and dose by gavage were modeled first. After determination of the appropriate PK model, the other cohort that received PBO through chow was added. The dose of PBO from chow was estimated using the amount of chow consumed by weight. The PBO content of the ingested chow per day was coded in three ways because of uncertainty about the rate at which the chow was consumed over the light vs dark periods. These dosing assumptions were: 1) daily amount of PBO ingested divided by 24 h, assuming constant eating rate; 2) daily amount of PBO ingested divided by 12 h to establish a dosing "rate" over only the dark period; 3) 30 % of daily chow consumption assumed to occur during the light cycle, with 70 % being consumed in the dark cycle [27]. If chow was measured after several days, the overall dose was distributed equally over these days. Assumption #1 that all chow was consumed continuously while available provided improved convergence compared to the other two dosing assumptions. The gavage dose in olive oil was set as the reference bioavailability of 100 %. It was learned after shipment and use that PBO-chow was inadvertently formulated by the contractor in two variations of base composition. Serum was collected from only four animals receiving the second lot of chow with one blood sample drawn from each, so no comparison of bioavailability could be made between the two lots of chow.

Because of rapid absorption and the lack of sufficient early sampling after gavage or early in the dark cycle, it was not possible to estimate an absorption rate of PBO from the gut, so ADVAN2 and ADVAN4 subroutines were discarded. Instead, the dose was initially assumed to be delivered directly into the central, sampled compartment (blood), and ADVAN1, ADVAN3, and ADVAN6 were used to test the simpler model. Tissue concentrations were available from some animals in the chow-dosed group, but only one animal dosed by gavage. Most samples were collected early during the dark cycle, but including the dark versus light cycle did not serve as a useful covariate in the PK model. The M3 approach for incorporating data points below quantifiable levels was tested, but did not improve the ability to fit the data [28].

Between subject (inter-individual) variability (IIV) was assessed on each PK parameter using an exponential model. Residual error was modeled as an additive error on the log scale, resulting in a proportional error model, although a combined proportional and additive error mode was also tested with less satisfactory results.

Selection of the structural model was made by inspection of residual error plots, NPDE distributions, and visual prediction charts (VPC), as well as by minimization of the objective function. A decrease in the OBJ value of $\geq$ 3.84 was considered a significant (p < 0.05) improvement by the addition of a covariate term. Model selection also included consideration of the condition number, calculated as the square root of the ratio of the highest and lowest values of the Eigen matrix from the covariance step. Although a condition number less than 20 was sought, condition numbers less than 100 were considered to have acceptable levels of co-linearity.

2.5.3. Covariate and error model development

Covariates that significantly contributed to the model when added singly were sought in a manner similar to that used to develop the structural model. These covariates were then all added to the model and individually removed to determine their impact upon the model. In addition to reductions in the objective function, the residual plots of the NPDE and IIV vs covariate were inspected for evidence of a covariate effect. Further, available demographic and laboratory covariates were added to the structural model to determine if the objective function and residual plots were improved.

2.5.4. Model evaluation

The relative bioavailability of PBO in olive oil administered by gavage at known time points was given a value of 1 in the initial model development, and inter-individual variation was successfully applied to the oral clearance and oral distribution volume.

The linear, one-compartment model was then applied to the entire dataset that included mice from which blood samples had been taken after either gavage or chow dosing with PBO. For the combined dataset the inter-individual variation term was placed on the relative bioavailability term F for mice dosed by gavage or chow. The values of clearance and distribution parameters were fixed at those that were obtained from the gavage-only treatment group. As illustrated in Table 2, combined dosing model with all data agreed with the results of the PK fit for gavage dosing.

Five hundred bootstrap runs were performed using the BOOTSTRAP process in NONMEM to provide 90 % confidence intervals for the parameters. The bootstrap test proved to be unstable with low accuracy (low significant figures). Instead, a visual prediction comparison (VPC) was made between the observed and simulated PBO concentrations using the final PK model (Fig. S1).

3. Results

To model acute exposure, female C57BL/6J mice were administered a single dose of 22.22 mg/kg, 66.67 mg/kg, 200 mg/kg, 600 mg/kg, or 1800 mg/kg PBO suspended in olive oil via oral gavage. Signs of overt toxicity were not observed in any of the dose groups. Serum PBO concentrations over time are depicted in Fig. 1. In the highest dose group, two concentration peaks were observed within 18 h, and serum levels remained readily detectable 48 h after acute exposure. In the other dose groups, maximum concentrations were observed within 12 h of administration. In the 200 mg/kg dose group, an additional concentration peak was observed prior to 24 h after administration, but by 48 h, concentrations were below the limit of quantification (LOQ). In the 22.22 and 66.67 mg/kg groups, serum PBO concentrations fell near the LOQ by 36 h after administration. When normalized to dose (Fig. 1C), serum concentrations of PBO were noted to be generally similar after gavage doses with the exception of the highest dose group (1800 mg/kg).

To model dietary exposure, female C57BL/6J mice were given chow containing 0.09 % PBO for eight days. Experimental diets were introduced one hour prior to the onset of the dark cycle on day zero. Chow consumption was similar between the control and PBO-containing diet over the experimental period (Fig. S2). Serum samples were collected at three daily time points during the eight-day period in which PBO-

containing diet was provided, four hours into the dark cycle, four hours into the light cycle, and just prior to the onset of the dark cycle. Additional serum samples were collected at the onset of the dark cycle 1-, 2-, and 4-days following return to control diet.

Serum PBO concentrations from dietary exposure are shown in Fig. 2A. The maximum serum PBO concentration was observed at the first sampling point five hours following introduction of PBO into the diet and four hours into the dark cycle. Subsequent serum concentrations generally followed a diurnal cycle, with concentrations higher during the dark cycle and lower during the light cycle. Serum PBO concentrations fell to near the LOQ within 24 h of removal of PBO-containing chow and by 96 h were below the LOQ (not shown).

Visceral adipose samples were also collected just prior to onset of the dark cycle to facilitate comparison to serum concentrations. During the 8-day experimental period of dietary PBO exposure, PBO concentrations detected in visceral adipose greatly exceeded those observed in the serum (Fig. 2B). Mean concentrations observed in visceral adipose tissue remained relatively consistent across the 8-day period of PBO exposure. When PBO-containing chow was removed, PBO content in the visceral adipose rapidly declined. Adipose PBO concentrations were markedly lower within 24 h of return to control diet but remained above the LOQ at 96 h.

3.1. Pharmacokinetic model

The final model for PBO in serum following oral administration was a linear one-compartment model. Gavage doses of PBO in olive oil were given fixed bioavailability values of 1. The limited number of subjects and sampling strategy impaired the ability to estimate Ka, so dosing was assumed to occur directly to the blood. Three animals receiving the highest gavage doses showed increasing serum PBO concentrations 12 h after the dose that were not explained by the successful PK models. These animals were excluded from the model because no reason could be found to dismiss the unexpected concentrations.

Few covariates were available to test for inclusion in the PK model. Adding mouse weight did not improve the fit, and in the end no covariates were included in the PK model of gavage dosing. The elimination half-life of PBO in the mouse after gavage dosing was 6.5 h (geometric mean, 90 % CI 4.7 – 9.5), and systemic oral clearance was 83.3 ± 20.5 mL/h (mean ± SE). As illustrated in Supplemental Fig. S1, the visual predictive check plot of simulated data points using the PK model agrees well with observed PBO concentrations. The PK model yielded an oral distribution volume of 791 mL for PBO in the mouse. Given a blood volume of approximately 2 mL in a 20 g mouse [29], this would suggest that the bioavailability of PBO in the mouse is only 0.25 %. The PK model also suggests that the bioavailability in chow was approximately 41 % relative to the gavage dosing in olive oil.

4. Discussion

The objective of this study was to establish a PK model of acute and dietary oral PBO exposure paradigms previously associated with adverse developmental outcomes in rodent models. The serum concentrations of PBO were best fit by a linear, one-compartment model. Noteworthy in Fig. 1 are double concentration peaks after gavage dosing of PBO. The peaks in PBO concentration appear at 2–3 h and approximately 8–12 h after the gavage dose, suggesting enterohepatic recirculation. Enterohepatic recirculation of PBO could not be modeled with the sparse sampling available. As illustrated in Fig. 1C, the dose-normalized PBO concentrations after the highest dose (1800 mg/kg) tended to be higher than those after the lower doses. The maximum observed concentration appeared somewhat later for the 1800 mg/kg dose, and the elimination slope shallower than for lower doses. Maximum observed values and elimination slopes for lower doses were similar. These results suggest that there may be slower elimination of PBO at the highest dose level and resulting concentrations that could be explained by a mixed-order

Table 2
Parameter estimates for final pharmacokinetic model.

Parameter	Gavage Doses Typical Mean (%CV)	Chow and Gavage Doses Typical Mean (%CV)
CL (mL/h)	83.3 (20.5)	83.3 FIXED
V (mL)	791 (20.5)	791 FIXED
F_{gavage}	1 FIXED	1 FIXED
F_{chow}	N/A	0.409 (20.6)
IIV CL	106.8 (15.4)	0
IIV V	96.7 (19.7)	0
IIV F_{gavage}	0	145 (15.2)
IIV F_{chow}	N/A	103 (20.7)
Proportional Residual Error	58.0 (12.9)	82.6 (9.8)

The oral bioavailability of the oral gavage dose in olive oil is assigned a value of 1. CL = Clearance, V = Distribution volume in central compartment, F_{chow} = Bioavailability relative to gavage dose, IIV = inter-individual variance on Parameter, CI = Confidence interval.
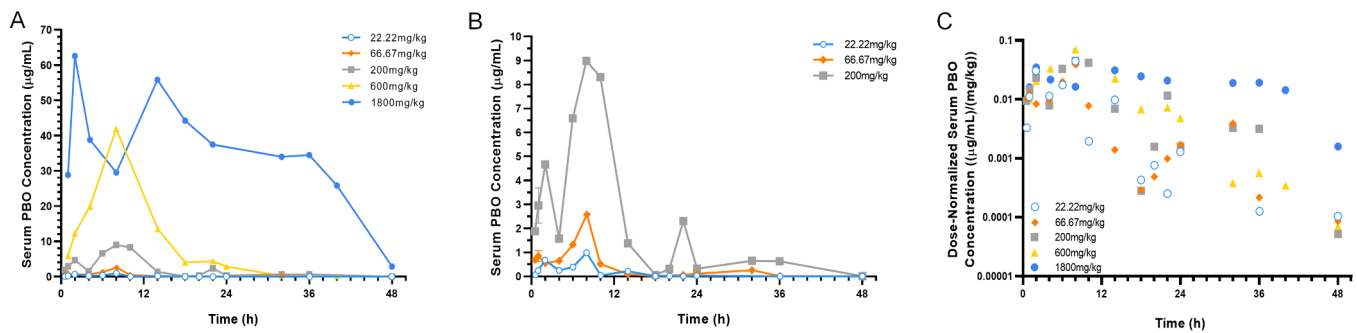
Fig. 1. Serum concentrations following acute PBO exposure. Wildtype non-pregnant C57BL/6J mice were administered the indicated dose of PBO by oral gavage. Serum samples were collected at indicated time points and PBO concentrations were measured by HPLC-MS/MS. Detected concentrations for all acute dose groups are plotted in (A), while concentrations for the three lower dose groups are plotted in (B). Dose-normalized concentrations over time are shown on a semi-log plot in (C). Each data point represents the exact value or mean of 2 independent samples.
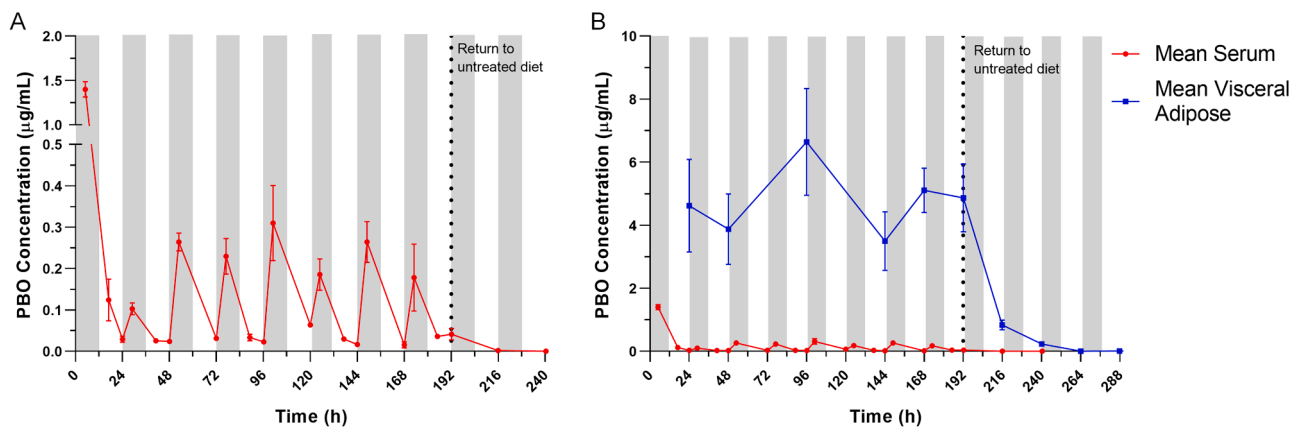
Fig. 2. Serum and visceral adipose concentrations following dietary PBO exposure. (A) Serum samples were collected at three daily time points: four hours into the dark cycle, four hours into the light cycle, and at the onset of the dark cycle over the eight-day period of dietary PBO exposure. Additional serum samples were collected at onset of the dark cycle 1-, 2-, and 4-days following return to control diet. Observed serum PBO concentrations over time in the 0.09 % dietary PBO group are plotted. Values represent the mean of 2–8 samples and error bars represent SEM. (B) Visceral adipose tissue was collected at the onset of the dark cycle during the eight-day period of dietary PBO exposure and for 4 days following return to control diet. Observed visceral adipose PBO concentrations over time in the 0.09 % dietary PBO group are plotted. Values represent the mean of 4–8 samples and error bars represent SEM. Mean serum concentrations from the 0.09 % dietary PBO group are also plotted for comparison. For both plots, gray shaded areas indicate dark cycle periods, while non-shaded areas indicate light cycle periods. Vertical dotted lines represent the transition from PBO-containing diet to control untreated diet.

PK model with partial saturation of clearance. However, the sparse sampling of serum in these mice precluded a confident selection of a mixed-order PK model over the final first-order (linear) model that would explain the somewhat disparate results of the 1800 mg/kg dose.

PBO is relatively lipophilic with reported logP values between 4.60 and 4.95 [3,30]. In the present study, pilot assays on tissue from a single mouse collected four hours following acute oral exposure to 600 mg/kg PBO suggested that PBO concentration in visceral adipose exceeded serum concentration by approximately four-fold (Fig. S3). Based upon this initial observation, visceral adipose tissue was more rigorously sampled in the dietary exposure model. We found that PBO concentrations in visceral adipose tissue greatly exceeded serum concentrations (Fig. 2), demonstrating that PBO readily distributes to adipose tissue. However, adipose concentrations did not accumulate over the eight-day period of dietary exposure. Upon return to control diet, adipose PBO concentrations decreased relatively quickly but remained detectable four days later. These observations are consistent with previous findings from studies examining oral PBO exposure in rats. One study found that 64.1–85 % of PBO was excreted within 48 h of administration [31], while another found that PBO concentration in adipose remained detectable 96 h after administration of a single 250 mg/kg dose [23]. Taken together, these findings suggest that although PBO readily distributes to adipose, this tissue does not represent a significant reservoir

of PBO following cessation of exposure.

PBO acts as an insecticide synergist by inhibiting insect CYP enzymes. Studies in rats and mice have demonstrated that PBO, particularly when administered at high doses, also inhibits the activity of mammalian oxidative enzymes, including CYPs, and can prolong the activity of other drugs metabolized by these enzymes [32–40]. Additional evidence demonstrates that PBO can induce CYP activity and may elicit a biphasic effect in which CYP inhibition by PBO is followed by CYP induction [41–45]. Metabolism of PBO itself is also incompletely understood, but existing animal studies demonstrate that it undergoes extensive oxidative metabolism, suggesting involvement of CYP enzyme activity [22,31]. That PBO both regulates CYP activity, and is itself likely metabolized by the same class of enzymes may have PK implications and contribute to observations in the present study. We observed that dose-normalized PBO concentrations after the highest acute dose (1800 mg/kg) tended to be higher than those after the lower doses (Fig. 1C). This would suggest that at higher drug concentrations there may exist saturable elimination of PBO. In contrast, in the PBO diet exposure model in which peak PBO serum concentrations were approximately 40-fold lower than for the 1800 mg/kg acute dose (Fig. 1A vs Fig. 2), the maximum serum PBO concentration was observed within the first 24 h of exposure to PBO-chow, and then on subsequent days was approximately 5-fold lower (Fig. 2). This drop in peak

concentrations may represent metabolizing enzyme induction not noted in the single dose gavage conditions. These observations may provide important context for comparison of studies examining the impact of a single acute PBO dose versus those examining daily acute or chronic dietary exposure.

Renewed interest in PBO stems in part from its discovery as an inhibitor of the Shh signaling pathway and recent mouse and zebrafish studies suggesting that PBO can cause developmental toxicity through Shh pathway inhibition [8,13,46]. The dosing paradigms evaluated in this study were selected to parallel those reported to cause adverse developmental outcomes in previous rodent studies [8–12]. Our previous study examining the impact of acute *in utero* PBO exposure in the mouse identified a lowest observable effect level of 66.67 mg/kg. In the present study, the same dose of 66.67 mg/kg yielded a maximum observed serum PBO concentration of approximately 2.58 μg/mL (7.62 μM). The dietary concentration of 0.09 % PBO was chosen based upon previous studies demonstrating an impact of dietary PBO exposure on mouse behavior [10]. In the present study, dietary exposure of 0.09 % PBO yielded an initial peak concentration of PBO of approximately 1.40 μg/mL (4.14 μM), with subsequent peak observed concentrations between 0.2 and 0.4 μg/mL (0.59–1.18 μM). 2D and 3D mammalian cell culture systems previously identified EC_{50} values of 0.22 μM and 1.62 μM for PBO-mediated inhibition of Shh pathway activity [13,47]. Taken together, these observations suggest that PBO dosing regimens that cause adverse developmental outcomes in rodents produce peak serum concentrations approximating or exceeding those that are sufficient to inhibit the Shh signaling pathway.

The present study was constrained by several limitations. Wildtype C57BL/6J mice were utilized because this is the most widely implemented inbred mouse strain in biomedical research, and the study was limited to female mice to extrapolate results to studies of maternal exposure and developmental toxicity. However, the use of relatively young and lean non-pregnant female mice presents limitations as pregnancy is associated with alterations in CYP enzyme expression [48, 49] and obesity may impact pharmacokinetics, particularly for lipophilic drugs [50–52]. Whether pregnancy or obesity impact PBO pharmacokinetics are important questions that should be addressed in future investigations. Several limitations in developing the PBO PK model are also noteworthy. Blood sampling to characterize the pharmacokinetics of orally-administered PBO was limited to 3–4 samples per mouse. Although the use of inbred strains of mice such as C57BL/6J may improve inter-animal consistency of PK parameters, variations in absorption and rate of chow ingestion are likely and would lead to substantial inter-animal variability in PK parameters. The number of samples drawn soon after the gavage doses was small, obstructing the ability to assess the rate of gastric absorption of PBO in mice. It was of interest that there was a poor correlation between serum and concurrent tissue (visceral fat) concentrations of PBO up to several days after the removal of PBO-containing chow (Fig. 3). This lack of correlation prevented a 2-compartment model fitting from incorporating measured tissue concentrations. The central oral distribution volume (V) was approximately 40-fold higher than the animal weight, suggesting that the absolute bioavailability of PBO in both oil and chow was very low. This is because the apparent distribution volume after an oral dose is determined by V/F, where V is the actual central distribution volume, and F is the absolute bioavailability.

5. Conclusions

In summary, HPLC-MS/MS was utilized to define PBO concentrations in serum and adipose tissue following its administration by acute oral gavage or dietary exposure in mice. We found that PBO dosing paradigms associated with adverse developmental outcomes in the mouse produce peak serum concentrations corresponding to those sufficient to inhibit the Shh signaling pathway in previously reported cell-based assays. Serum PBO concentrations were best fit by a linear, one-
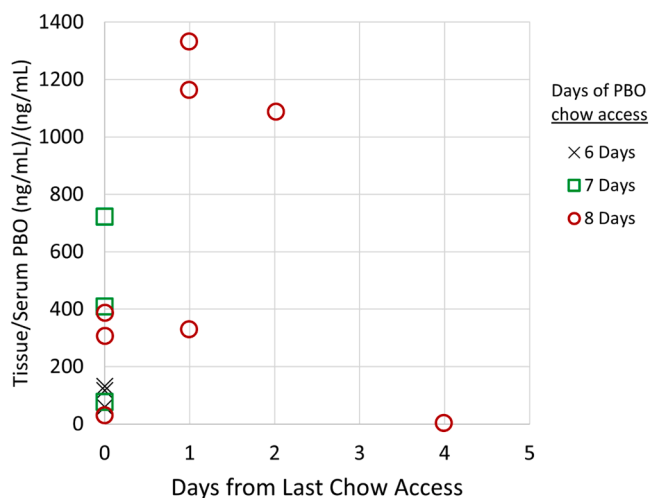

Fig. 3. Comparison of adipose and serum PBO concentrations. Concentrations of PBO in visceral adipose tissue are compared to contemporary serum PBO concentrations. The x-axis indicates number of days since removal of PBO-containing chow, with values at 0 collected from animals remaining on PBO-containing chow at time of tissue collection. Plot symbols indicate the number of days individual animals were on PBO-containing diet prior to sample collection.

compartment model, and PBO concentrations detected in adipose greatly exceed serum concentrations. The relatively rapid elimination of PBO suggests exposure avoidance as a useful approach to mitigate potential human health risks.

CRediT authorship contribution statement

A.E. Jenkins, C.O. Scarlett, P.R. Hutson, and **R.J. Lipinski** conceived and designed the experiments. A.**E. Jenkins, C.O. Scarlett, T.G. Beames, K.S. Rivera-Gonzalez, M.R. Sun**, and **A.A. Martin** performed the experiments. **A.E. Jenkins C.O. Scarlett**, and **P.R. Hutson** analyzed the data. **R.J. Lipinski** acquired financial support. **A.E. Jenkins, T.G. Beames, P.R. Hutson**, and **R.J. Lipinski** wrote the manuscript draft. **C.O. Scarlett, K.S. Rivera-Gonzalez**, and **M.R. Sun** revised the manuscript. All authors participated in reading and agreed to the final version of the manuscript.

Declaration of Competing Interest

The authors declare that they have no known competing financial interests or personal relationships that could have appeared to influence the work reported in this paper.

Data availability

Data will be made available on request.

graphical abstract was created with BioRender.com.

Appendix A. Supporting information

Supplementary data associated with this article can be found in the online version at doi:10.1016/j.toxrep.2023.09.017.

References

[1] D.G. Jones, Piperonyl Butoxide, Elsevier, 1998.
[2] A. Cross, C. Bond, K. Buhl, J. Jenkins. Piperonyl Butoxide General Fact Sheet 2017, National Pesticide Information Center, Oregon State University Extension Services, 2017.
[3] R. Daiss, D. Edwards, Reregistration Eligibility Decision for Piperonyl Butoxide (RED), Office of Pesticide Programs, United States Environment Protection Agency, Washington, D.C, 2006.
[4] K.S. Khera, C. Whalen, G. Angers, G. Trivett, Assessment of the teratogenic potential of piperonyl butoxide, biphenyl, and phosalone in the rat, Toxicol. Appl. Pharmacol. 47 (2) (1979) 353–358, https://doi.org/10.1016/0041-008X(79)90330-2.
[5] G.L. Kennedy, S.H. Smith, F.K. Kinoshita, M.L. Keplinger, J.C. Calandra, Teratogenic evaluation of piperonyl butoxide in the rat, Food Cosmet. Toxicol. 15 (4) (1977) 337–339, https://doi.org/10.1016/S0015-6264(77)80207-1.
[6] A.M. Hoberman, J.W. Hauswirth, Developmental and reproduction toxicity of piperonyl butoxide part 1 developmental safety of piperonyl butoxide in the CD® (Sprague Dawley) rat, Reprod. Toxicol. 112 (2022) 171–176, doi: 10.1016/j.reprotox.2022.07.010.
[7] A.M. Hoberman, J.W. Hauswirth, Developmental and reproduction toxicity of piperonyl butoxide part 2 developmental safety of piperonyl butoxide in the NZW rabbit, Reprod. Toxicol. 112 (2022) 177–181, doi: 10.1016/j.reprotox.2022.07.009.
[8] J.L. Everson, M.R. Sun, D.M. Fink, G.W. Heyne, C.G. Melberg, K.F. Nelson, et al., Developmental toxicity assessment of piperonyl butoxide exposure targeting sonic hedgehog signaling and forebrain and face morphogenesis in the mouse: an in vitro and in vivo study, Environ. Health Perspect. 127 (10) (2019), 107006, https://doi.org/10.1289/EHP5260.
[9] T. Tanaka, T. Fujitani, O. Takahashi, S. Oishi, Developmental toxicity evaluation of piperonyl butoxide in CD-1 mice, Toxicol. Lett. 71 (2) (1994) 123–129, https://doi.org/10.1016/0378-4274(94)90172-4.
[10] T. Tanaka, A. Inomata, Effects of maternal exposure to piperonyl butoxide (PBO) on behavioral development in F1-generation mice, Birth Defects Res B Dev. Reprod. Toxicol. 104 (6) (2015) 227–237, doi: 10.1002/bdrb.21163.
[11] T. Tanaka, T. Fujitani, O. Takahashi, S. Oishi, M. Yoneyama, Developmental toxicity study of piperonyl butoxide in CD rats, Toxicol. Ind. Health 11 (2) (1995) 175–184, doi: 10.1177/074823379501100205.
[12] T. Tanaka, A. Inomata, Reproductive and neurobehavioral effects of maternal exposure to piperonyl butoxide (PBO) in F, Birth Defects Res B Dev. Reprod. Toxicol. 107 (4–5) (2016) 195–205, doi: 10.1002/bdrb.21185.
[13] J. Wang, J. Lu, R. Mook, M. Zhang, S. Zhao, L. Barak, et al., The insecticide synergist piperonyl butoxide inhibits Hedgehog signaling: assessing chemical risks, Toxicol. Sci. 128 (2) (2012) 517–523, https://doi.org/10.1093/toxsci/kfs165.
[14] C. Chiang, Y. Litingtung, E. Lee, K.E. Young, J.L. Corden, H. Westphal, et al., Cyclopia and defective axial patterning in mice lacking Sonic hedgehog gene function, Nature 383 (6599) (1996) 407–413, https://doi.org/10.1038/383407a0.
[15] G.W. Heyne, C.G. Melberg, P. Doroodchi, K.F. Parins, H.W. Kietzman, J.L. Everson, et al., Definition of critical periods for Hedgehog pathway antagonist-induced holoprosencephaly, cleft lip, and cleft palate, PLoS One 10 (3) (2015), e0120517, https://doi.org/10.1371/journal.pone.0120517.
[16] K.S. Rivera-González, T.G. Beames, R.J. Lipinski, Examining the developmental toxicity of piperonyl butoxide as a Sonic hedgehog pathway inhibitor, Chemosphere 264 (Pt 1) (2021), 128414 doi: 10.1016/j.chemosphere.2020.128414.
[17] R.A. Rudel, D.E. Camann, J.D. Spengler, L.R. Korn, J.G. Brody, Phthalates, alkylphenols, pesticides, polybrominated diphenyl ethers, and other endocrine-disrupting compounds in indoor air and dust, Environ. Sci. Technol. 37 (20) (2003) 4543–4553, https://doi.org/10.1021/es0264596.
[18] M.B. Woudneh, D.R. Oros, Quantitative determination of pyrethroids, pyrethrins, and piperonyl butoxide in surface water by high-resolution gas chromatography/high-resolution mass spectrometry, J. Agric. Food Chem. 54 (19) (2006) 6957–6962, doi: 10.1021/jf0609431.
[19] G. Neta, L.R. Goldman, D. Barr, A. Sjödin, B.J. Apelberg, F.R. Witter, et al., Distribution and determinants of pesticide mixtures in cord serum using principal component analysis, Environ. Sci. Technol. 44 (14) (2010) 5641–5648, https://doi.org/10.1021/es1009778.
[20] S. Selim, F.J. Preiss, K.L. Gabriel, J.H. Jonkman, T.G. Osimitz, Absorption and mass balance of piperonyl butoxide following an 8-h dermal exposure in human volunteers, Toxicol. Lett. 107 (1–3) (1999) 207–217, https://doi.org/10.1016/s0378-4274(99)00049-1.
[21] J.E. Casida, J.L. Engel, E.G. Essac, F.X. Kamienski, S. Kuwatsuka, Methylene-C14-dioxyphenyl compounds: metabolism in relation to their synergistic action, Science 153 (3740) (1966) 1130–1133, https://doi.org/10.1126/science.153.3740.1130.
[22] F.X. Kamienski, J.E. Casida, Importance of demethylenation in the metabolism in vivo and in vitro of methylenedioxyphenyl synergists and related compounds in

mammals, Biochem. Pharmacol. 19 (1) (1970) 91–112, https://doi.org/10.1016/0006-2952(70)90331-X.
[23] R. Kimura, H. Deguchi, T. Murata, Absorption distribution and excretion of piperonyl butoxide in rats, Food Hyg. Saf. Sci. (Shokuhin Eiseigaku Zasshi) 24 (3) (1983) 319–23_1.
[24] D.R. Mould, R.N. Upton, Basic concepts in population modeling, simulation, and model-based drug development, CPT Pharmacomet. Syst. Pharmacol. 1 (2012), e6.
[25] D.R. Mould, R.N. Upton, Basic concepts in population modeling, simulation, and model-based drug development-part 2: introduction to pharmacokinetic modeling methods, CPT Pharmacomet. Syst. Pharmacol. 2 (2013), e38.
[26] E.N. Jonsson, M.O. Karlsson, Xpose–an S-PLUS based population pharmacokinetic/pharmacodynamic model building aid for NONMEM. Comput. Methods Prog. Biomed. 58 (1) (1999) 51–64, https://doi.org/10.1016/s0169-2607(98)00067-4.
[27] K.L. Ellacott, G.J. Morton, S.C. Woods, P. Tso, M.W. Schwartz, Assessment of feeding behavior in laboratory mice, Cell Metab. 12 (1) (2010) 10–17, https://doi.org/10.1016/j.cmet.2010.06.001.
[28] S.L. Beal, Ways to fit a PK model with some data below the quantification limit, J. Pharmacokinet. Pharmacodyn. 28 (5) (2001) 481–504, https://doi.org/10.1023/a:1012299115260.
[29] A.C. Riches, J.G. Sharp, D.B. Thomas, S.V. Smith, Blood volume determination in the mouse, J. Physiol. 228 (2) (1973) 279–284, https://doi.org/10.1113/jphysiol.1973.sp010086.
[30] Tomlin C., British Crop Protection Council, The Pesticide Manual: a World Compendium, twelfth ed, British Crop Protection Council, Farnham, 2000. xxvi, 1250.
[31] J. Byard, D. Needham, Metabolism and excretion of piperonyl butoxide in the rat, Xenobiotica 36 (12) (2006) 1259–1272, https://doi.org/10.1080/00498250600856306.
[32] B.C. Fine, J.O. Molloy, Effects of insecticide synergists on duration of sleep induced in mice by barbiturates, Nature 204 (1964) 789–790, https://doi.org/10.1038/204789b0.
[33] M.W. Anders, Inhibition of microsomal drug metabolism by methylenedioxybenzenes, Biochem Pharmacol. 17 (11) (1968) 2367–2370, https://doi.org/10.1016/0006-2952(68)90046-4.
[34] K. Jaffe, H. Jaffe, S.S. Epstein, Factors influencing the hexobarbital sleeping time and zoxazolamine paralysis time in mice, Toxicol. Appl. Pharmacol. 13 (3) (1968) 431–438, https://doi.org/10.1016/0041-008x(68)90119-1.
[35] H. Jaffe, K. Fujii, M. Sengupta, H. Guerin, S.S. Epstein, In vivo inhibition of mouse liver microsomal hydroxylating systems by methylenedioxyphenyl insecticidal synergists and related compounds, Life Sci. 7 (19) (1968) 1051–1062, https://doi.org/10.1016/0024-3205(68)90211-7.
[36] H. Jaffe, J.L. Neumeyer, Comparative effects of piperonyl butoxide and N-(4-pentynyl)phthalimide on mammalian microsomal enzyme functions, J. Med Chem. 13 (5) (1970) 901–903, https://doi.org/10.1021/jm00299a024.
[37] M.R. Franklin, Inhibition of hepatic oxidative xenobiotic metabolism by piperonyl butoxide, Biochem Pharmacol. 21 (24) (1972) 3287–3299, https://doi.org/10.1016/0006-2952(72)90093-7. PubMed PMID: 4405369.
[38] M.A. Friedman, E.J. Greene, R. Csillag, S.S. Epstein, Paradoxical effects of piperonyl butoxide on the kinetics of mouse liver microsomal enzyme activity, Toxicol. Appl. Pharmacol. 21 (3) (1972) 419–427, https://doi.org/10.1016/0041-008x(72)90162-7.
[39] H.A. Benchaoui, Q.A. McKellar, Interaction between fenbendazole and piperonyl butoxide: pharmacokinetic and pharmacodynamic implications, J. Pharm. Pharmacol. 48 (7) (1996) 753–759, https://doi.org/10.1111/j.2042-7158.1996.tb03965.x.
[40] L. Xu, X. Xu, L. Guo, Z. Wang, X. Wu, H. Kuang, et al., Potential environmental health risk analysis of neonicotinoids and a synergist, Environ. Sci. Technol. 55 (11) (2021) 7541–7550, https://doi.org/10.1021/acs.est.1c00872.
[41] H.B. Matthews, M. Skrinjarić-Spoljar, J.E. Casida, Insecticide synergist interactions with cytochrome P-450 in mouse liver microsomes, Life Sci. I 9 (18) (1970) 1039–1048, https://doi.org/10.1016/0024-3205(70)90107-4.
[42] M. Skrinjarić-Spoljar, H.B. Matthews, J.L. Engel, J.E. Casida, Response of hepatic microsomal mixed-function oxidases to various types of insecticide chemical synergists administered to mice, Biochem Pharmacol. 20 (7) (1971) 1607–1618, https://doi.org/10.1016/0006-2952(71)90289-9.
[43] R.M. Philpot, E. Hodgson, The effect of piperonyl butoxide concentration on the formation of cytochrome P-450 difference spectra in hepatic microsomes from mice, Mol. Pharmacol. 8 (2) (1972) 204–214.
[44] M.R. Franklin, Methylenedioxyphenyl insecticide synergists as potential human health hazards, Environ. Health Perspect. 14 (1976) 29–37, https://doi.org/10.1289/ehp.761429.
[45] Hodgson E., Levi P.E. 3 - Interactions of piperonyl butoxide with cytochrome P450, in: Jones DG, (Ed.), Piperonyl Butoxide, Academic Press, London, 1999. 41-II.
[46] J.L. Everson, R. Batchu, J.K. Eberhart, Multifactorial genetic and environmental hedgehog pathway disruption sensitizes embryos to alcohol-induced craniofacial defects, Alcohol. Clin. Exp. Res. 44 (10) (2020) 1988–1996, doi: 10.1111/acer.14427.
[47] B.P. Johnson, R.A. Vitek, M.M. Morgan, D.M. Fink, T.G. Beames, P.G. Geiger, et al., A microphysiological approach to evaluate effectors of intercellular hedgehog signaling in development, Front. Cell Dev. Biol. 9 (2021), 621442, https://doi.org/10.3389/fcell.2021.621442.
[48] K.H. Koh, H. Xie, A.M. Yu, H. Jeong, Altered cytochrome P450 expression in mice during pregnancy, Drug Metab. Dispos. 39 (2) (2011) 165–169, doi: 10.1124/dmd.110.035790.
[49] N. Isoherranen, K.E. Thummel, Drug metabolism and transport during pregnancy: how does drug disposition change during pregnancy and what are the mechanisms

that cause such changes? Drug Metab. Dispos. 41 (2) (2013) 256–262, https://doi.org/10.1124/dmd.112.050245.

[50] C.D. Bruno, J.S. Harmatz, S.X. Duan, Q. Zhang, C.R. Chow, D.J. Greenblatt, Effect of lipophilicity on drug distribution and elimination: influence of obesity, Br. J. Clin. Pharm. 87 (8) (2021) 3197–3205, doi: 10.1111/bcp.14735.

[51] M. Weiss, How does obesity affect residence time dispersion and the shape of drug disposition curves? Thiopental as an example, J. Pharmcokinet. Pharmacodyn. 35 (3) (2008) 325–336, doi: 10.1007/s10928-008-9090-8.

[52] G. Cheymol, Effects of obesity on pharmacokinetics implications for drug therapy, Clin. Pharmacokinet. 39 (3) (2000) 215–231, https://doi.org/10.2165/00003088-200039030-00004.